Journal of Thermal Analysis and Calorimetry
https://doi.org/10.1007/s10973-018-7780-z

Thermal and electrical properties of $Ca_5Mg_{4-x}Zn_x(VO_4)_6$ ($0 \leq x \leq 4$)

Anna S. Tolkacheva[1,2] · Sergey N. Shkerin[1] · Kirill G. Zemlyanoi[2] · Olga G. Reznitskikh[3,4] · Svetlana V. Pershina[1] · Pavel D. Khavlyuk[2]

Received: 1 March 2018 / Accepted: 2 October 2018

Abstract
Calcium vanadates $Ca_5Mg_{4-x}Zn_x(VO_4)_6$ ($0 \leq x \leq 4$) have been studied for the first time using a set of high-temperature methods of analysis. The onset of melting process determined from differential scanning calorimetry decreases from 1158 to 881 °C (± 1.5 °C) with increasing of x (dopant's content). CTE temperature dependence is found to show a hysteresis. Electrical transport properties measured by impedance spectroscopy in air of different humidity are also discussed. The value of electrical conductivity does not depend on air humidity. It is found to equal to 1.5×10^{-6} S cm^{-1} at 720 °C for $Ca_5Mg_4(VO_4)_6$ which is specific for garnet-related crystals.

Keywords Non-stoichiometric garnet · Electrical conductivity · DSC · Thermal expansion

Introduction

Vanadate $Ca_5Mg_{4-x}Zn_x(VO_4)_6$ ($0 \leq x \leq 4$) belongs to the garnet-related family $A_5M_4(VO_4)_6$ (A = Ca, Na, K; M = Mg, Zn, Co, Ni, Mn) of multifunctional oxides that have recently attracted interest as luminescent materials, microwave dielectrics and magneto-dielectrics. Self-luminescent $Ca_5Mg_4(VO_4)_6$ and $Ca_5Zn_4(VO_4)_6$ vanadate garnets are intensively studied as rare elements-free broadband excitation and emission phosphors. These compounds are also considered promising for ultraviolet-based white light-emitting diodes (WLEDs) [1, 2]. $Ca_5M_4(VO_4)_6$ (M = Mg, Zn, Ni) are discussed as potential solids for application in microwave devices as substrate materials. Besides having low sintering temperatures, they demonstrate excellent microwave dielectric properties [3, 4]. This fact makes them perspective in such field of industry as low temperature co-fired ceramic (LTCC) [5] and even ultra-low temperature co-fired ceramic (ULTCC), for example, $Na_2BiZn_2V_3O_{12}$ [6] which is sintered at 600 °C.

$Ca_5Mg_{4-x}Zn_x(VO_4)_6$ has garnet-related non-centrosymmetric crystal structure with space symmetry $I\bar{4}3d$ [7]. The features of the crystal structure include dodecahedral coordination around the calcium atoms and octahedral for the magnesium and zinc atoms; vanadium atoms have tetrahedral coordination. $Ca_5Mg_{4-x}Zn_x(VO_4)_6$ has structural cavities arranging three-dimensional channels [7]. Another garnet-related material mayenite $Ca_{12}Al_{14}O_{33\pm\delta}$ having analogous space symmetry and positively charged framework is known as anti-zeolitic material [8]. The feature of its structure is a high deficiency in cationic and anionic sublattices which provides high anionic conductivity $\sim 10^{-2}$ S/cm above 900 °C [9, 10]. There are numerous compositions of vanadates having this structural type $(Ca_{2.5}\square_{0.5})M_2V_3O_{12-x}$ (M = Mg, Zn, Ni, Co, Mn; □—vacancy in A-sublattice in garnet $A_3B_2C_3O_{12}$). Their heightened cation deficiency in comparison with garnets having $Ia\bar{3}d$ space group is compensated by the increased number of oxygen vacancies to maintain electroneutrality. Therefore, $Ca_5Mg_{4-x}Zn_x(VO_4)_6$ is suspected to have oxygen ionic conductivity higher than classical garnet materials.

✉ Anna S. Tolkacheva
mail-content@mail.ru

[1] Institute of High-Temperature Electrochemistry, Ural Branch of Russian Academy of Sciences, 20, Akademicheskaya, Ekaterinburg, Russia 620137

[2] INMT Ural Federal University, Ekaterinburg, Russia 620002

[3] Institute of Solid State Chemistry, Ural Branch of Russian Academy of Sciences, Ekaterinburg, Russia 620990

[4] Inenergy Llc, Second Kotlyakovskiy Lane, 18, Moscow, Russia 115201

Published online: 13 October 2018

Whereas most studies on $Ca_5Mg_4(VO_4)_6$ and $Ca_5Zn_4(VO_4)_6$ are performed in the field of lighting technology and electronics, its thermal phase stability and electrical conductivity have not been studied yet. The goal of this study is to estimate these properties for $Ca_5Mg_{4-x}Zn_x(VO_4)_6$ solid solution by helps of simultaneous thermal analysis, dilatometry and impedance spectroscopy.

Experimental procedure

The sol–gel method was applied for the synthesis of the $Ca_5Mg_{4-x}Zn_x(VO_4)_6$ ($0 \le x \le 4$). Initial precursor materials for synthesis comprised: $CaCO_3$ (99%), $MgCO_3$ (99.999%), ZnO (99%), NH_4VO_3 (98%), HCOOH (98%, concentration 99%) and $C_6H_8O_7{\cdot}H_2O$ (99%). Ethanol was used as a grinding medium. The initial reagents at a stoichiometric ratio were dissolved in distilled water with HCOOH. Then $C_6H_8O_7{\cdot}H_2O$ was added with subsequent stirring and heating at 70–80 °C on a hot plate. Homogeneous water reagent solutions were slowly evaporated into a gel. Afterward, the as-prepared gel was placed into a furnace at 120 °C for 12 h. The formed xerogel was ground in a jasper mortar and calcined at 600 °C for 1 h. The powders were pressed into pellets and annealed in alumina crucibles with rest of the powder of the same chemical composition. Heat treatment of the samples was carried out as follows, heating up to 600 °C was performed at a rate of 200 °C/h and then up to 750–970 °C at a rate of 10 °C/h depending on chemical composition. Samples were treated in air for 48 h. The final products were checked by powder X-ray diffraction (XRD) on a Rigaku D/MAX-2200 X-ray diffractometer using Cu $K\alpha$ radiation in the 2θ range from 15° to 80° with a step of 0.02°. The absence of possible impurity phases was proved by comparing their XRD patterns with $Ca_5Mg_4(VO_4)_6$, $Ca_5Zn_4(VO_4)_6$ and $Ca_5Mg_3Zn(VO_4)_6$ in the FIZ ICSD database (2017).

Bulk samples for dilatometric and electrical measurements have been prepared as follows. Sintered polycrystalline powders were pressed under the hydraulic press with 2-ton pressure into pellets of 15 mm dia and 2 mm thickness for electrical measurements and bricks of $5 \times 5 \times 25$ mm for dilatometric study. Samples were heated at a temperature equal to 0.8 of melting point to obtain dense ceramics. The apparent density of samples was determined using Archimedes' principle and equals over 97% of theoretical value (Table 1).

Simultaneous thermal analysis (STA) including DSC/TG combination of differential scanning calorimetry and thermogravimetry of the calcium vanadates was carried out by a Netzch STA 449C Jupiter, using Pt crucibles in an air atmosphere and a temperature range from 35 to 1200 °C at a heating rate of 10 K min^{-1}. The STA measurements were performed on the bulk solid samples (10–20 mg) directly after annealing. Coefficients of thermal expansion (CTE), denoted by the symbol α, which is the slope of $\Delta L/L_o$ versus temperature at constant pressure, were measured by a Netzsch 402PC dilatometer in air atmosphere up to

Table 1 Onset of melting points of $Ca_5Mg_{4-x}Zn_x(VO_4)_6$ compounds

x	Composition	Melting point/°C	Apparent density/ g cm^{-3}
0	$Ca_5Mg_4(VO_4)_6$	1158 ± 1.5	3.30 ± 0.02
1	$Ca_5Mg_3Zn(VO_4)_6$	977 ± 1.5	3.28 ± 0.02
2	$Ca_5Mg_2Zn_2(VO_4)_6$	937 ± 1.5	3.46 ± 0.02
3	$Ca_5MgZn_3(VO_4)_6$	915 ± 1.5	3.60 ± 0.02
4	$Ca_5Zn_4(VO_4)_6$	881 ± 1.5	3.67 ± 0.02

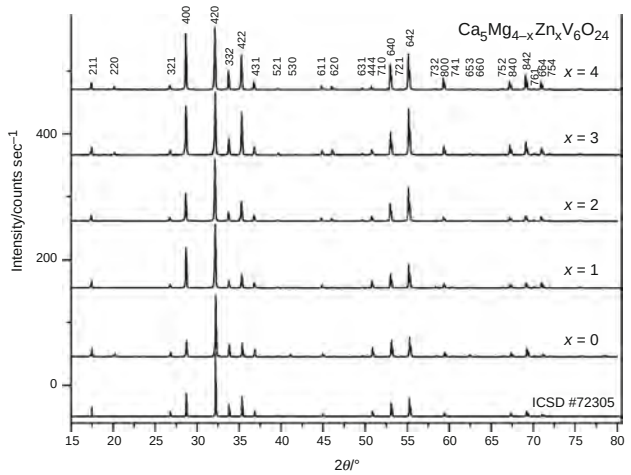

Fig. 1 X-ray patterns of powdered samples $Ca_5Mg_{4-x}Zn_x(VO_4)_6$ ($0 \le x \le 4$)

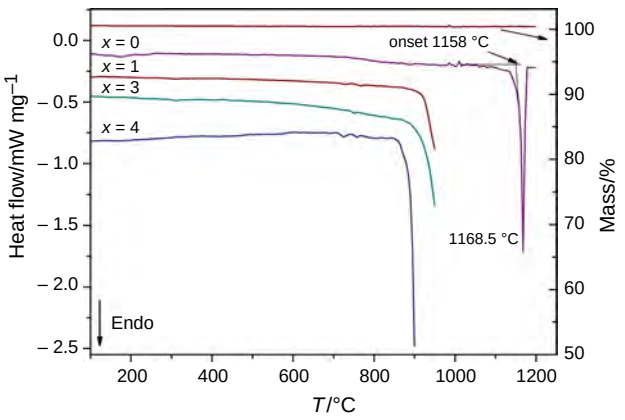

Fig. 2 DSC signals of $Ca_5Mg_{4-x}Zn_x(VO_4)_6$

900 °C at a heating rate of 1 K min^{-1}. The cycle of dilatometry measurements at heating and cooling was carried out three times and showed well reproducibility. The data obtained were processed using the Netzch Proteus software.

Impedance spectra were obtained via the two-probe technique with an impedance meter Parstat 2273. Each sample was placed between platinum current collectors. Frequency range was from 1 MHz to 10 mHz and the amplitude of sinusoidal disturbance was 10 mV. Measurements were carried out in dry air (zeolite at room temperature, pH_2O = 0.04 kPa) and wet air atmosphere (pH_2O = 3.35 kPa) in the temperature range of 540–660 °C. The measurement technique was changed as described below for the temperature range from 660 to 720 °C. Samples at every measurement step were heated at 20 °C higher than the previous measurement temperature and when they maintain equilibrium electrical

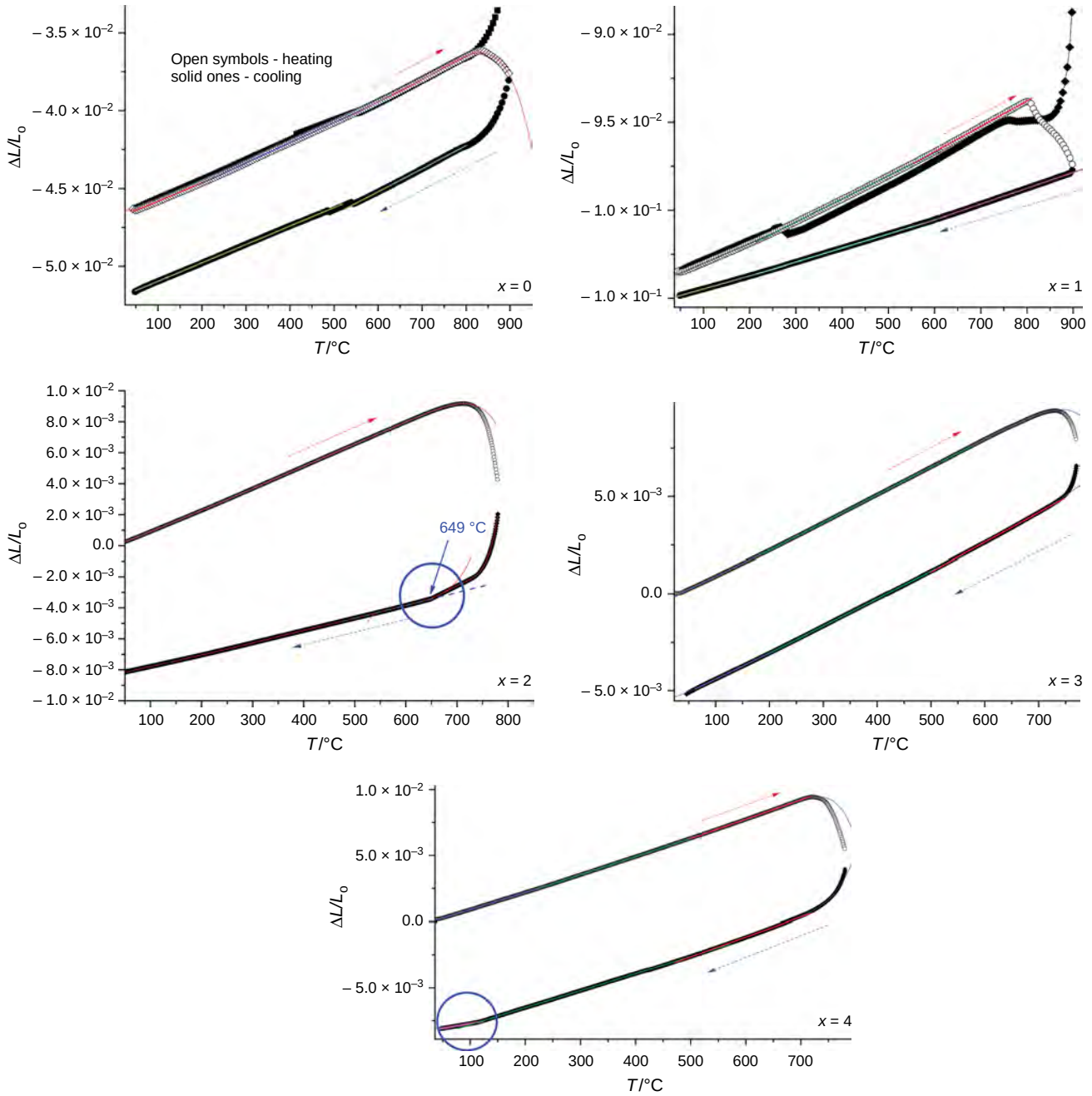

Fig. 3 Thermal expansion curves of $Ca_5Mg_{4-x}Zn_x(VO_4)_6$ in the temperature range of 30–850 °C in the air (black symbols—experiment data, colored curves—fitting), red arrow shows heating and blue arrow shows cooling. (Color figure online)

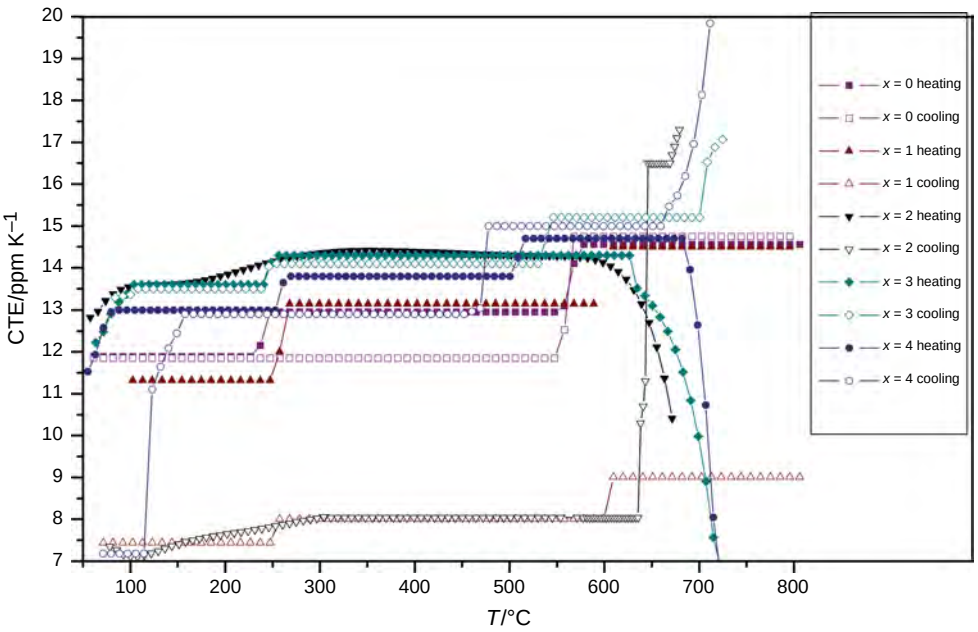

Fig. 4 CTE curves of $Ca_5Mg_{4-x}Zn_x(VO_4)_6$ as the function of temperature

Table 2 Coefficient of thermal expansion of $Ca_5Mg_{4-x}Zn_x(VO_4)_6$ at heating and cooling

Composition	Temperature range/°C	α, 10^6/K (at heating)	α, 10^6/K (at cooling)
$Ca_5Mg_4(VO_4)_6$	25–250	11.89	11.89
	250–550	12.96	11.85
	550–800	14.56	14.56
$Ca_5Mg_3Zn(VO_4)_6$	25–250	11.32	7.44
	250–550	13.14	8.00
	550–800	14.50	9.00
$Ca_5Mg_2Zn_2(VO_4)_6$	25–250	13.60	7.70
	250–550	14.40	8.00
	550–800	14.40	8.00
$Ca_5MgZn_3(VO_4)_6$	25–250	13.60	13.50
	250–550	14.30	14.10
	550–800	14.30	15.20
$Ca_5Zn_4(VO_4)_6$	25–250	13.00	7.18
	250–550	13.80	12.90
	550–800	14.70	15.00

measurements were made. After that samples were cooled to 660 °C and measured again. Such a cycle was repeated with increasing of temperature at every heating step with cooling to 660 °C every time. Such an approach allows us to exclude the shift in conductivity values caused by samples inelastic deformation by comparison with measurement results at the control point at 660 °C.

Results and discussion

Figure 1 shows the XRD patterns of $Ca_5Mg_{4-x}Zn_x(VO_4)_6$ ($0 \leq x \leq 4$) powders sintered from 800 to 1100 °C for 120 h. The observed peaks match well with the standard ICSD Card of $Ca_5Mg_3Zn(VO_4)_6$ no. 72305, no additional peaks are observed.

The important purpose of this work was to estimate thermal stability for $Ca_5Mg_{4-x}Zn_x(VO_4)_6$ solid solution.

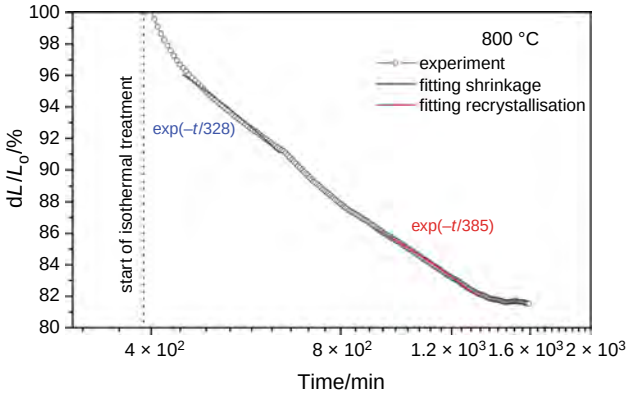

Fig. 5 Sintering behavior of $Ca_5Mg_3Zn(VO_4)_6$ at isothermal treatment at 800 °C. Time axis marks the overall time of experiment from the start of a heating process. Exp($-t$/328) and exp($-t$/385) denote the slope of a fitting curve

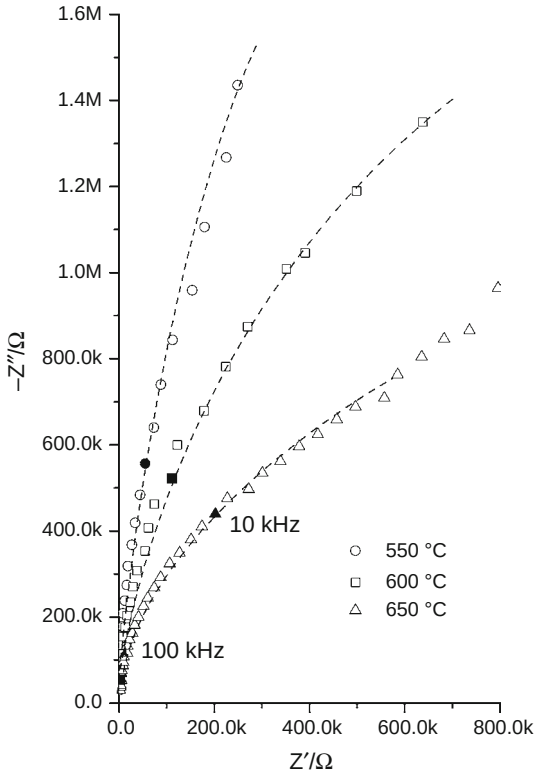

Fig. 6 Typical impedance spectra for $Ca_5Mg_4(VO_4)_6$ at temperatures 550, 600 and 650 °C

According to TG data (Fig. 2) for all the samples, the change in the mass of the samples during the heating up to the melting point does not exceed 0.15%. Since vanadate melts can react with crucible material and show high volatility [11], almost all measurements were made only up to the melting points. Melting point T_m is the point of intersection of the leading edge of a melting peak with the extrapolated baseline. Figure 2 depicts DSC curves of the $Ca_5Mg_{4-x}Zn_x(VO_4)_6$ solid solutions. It can be seen that all the samples reveal one endothermic effect of high enthalpy corresponding to the melting point. The values of melting temperatures are given in Table 1. As can be seen from the data obtained that an increase of the Zn^{2+} content in the solid solutions leads to the monotonic decrease of the T_m value in the entire range of the solid solution according to Schroder-Van Laar equation [12]. DSC curves demonstrate low energy disturbances near 700 °C corresponding to dilatometric softening of samples which is observed from thermal expansion curves (Fig. 3).

Dilatometric curves of almost samples demonstrate steps whereas dopant addition smoothes them. It can be seen that the slope of heating and cooling lines differs for samples containing x from 0 to 3 (Fig. 3). Nevertheless, the tendency to have a hysteresis of CTE is observed for almost all compounds of the solid solution.

CTE curves as a function of the temperature demonstrate two steps independently of samples composition near 250 °C and 450–650 °C (Fig. 4). The second step in CTE thermal dependence corresponds to small thermal effects on the DSC curve (the difference in 50 °C is a result of the different heating rate of these two methods). The coefficient of thermal expansion increases with the increase in dopant concentration Zn^{2+} having ionic radius larger than magnesium ions (Table 2). It is interesting that samples demonstrate CTE about 8×10^{-6} K^{-1} during cooling process near room temperature, whereas they are characterized by CTE value near 13×10^{-6} K^{-1} at heating.

Time dependence of samples shrinkage at isothermal treatment at 800 °C for $Ca_5Mg_3Zn(VO_4)_6$ (Fig. 5) demonstrates two steps. The first one has relaxation time equal to 6 h and is referred to isothermal shrinkage process. Another one begins on 13 h and achieves saturation during 2000 min. This effect is caused by the recrystallization process. The tendency to recrystallization for vanadate compounds is observed in [3].

Figure 6 represents the typical impedance spectra for $Ca_5Mg_4(VO_4)_6$ which confirms the dielectric nature of samples. A few cycles of electrical conductivity measurements from 660 to 540 °C in dry and wet air atmosphere performs almost identical results. They are represented in Arrhenius plots in Fig. 7 from which one can conclude that samples demonstrate hopping transfer mechanism of electrical conductivity. The activation energy at the intermediate temperature is about 100 ± 16 kJ mol^{-1} and taking into account a temperature range of experiment we conclude that charge carriers are electrons. The activation energy of electrical conductivity above 660 °C is higher and is estimated equal to 278(6) kJ mol^{-1} which indicates that oxygen anions could also impact in charge transfer. It is established that the humidity does not influence the conductivity of the samples (Fig. 7). This is a qualitatively new result, since the main problem of the previously

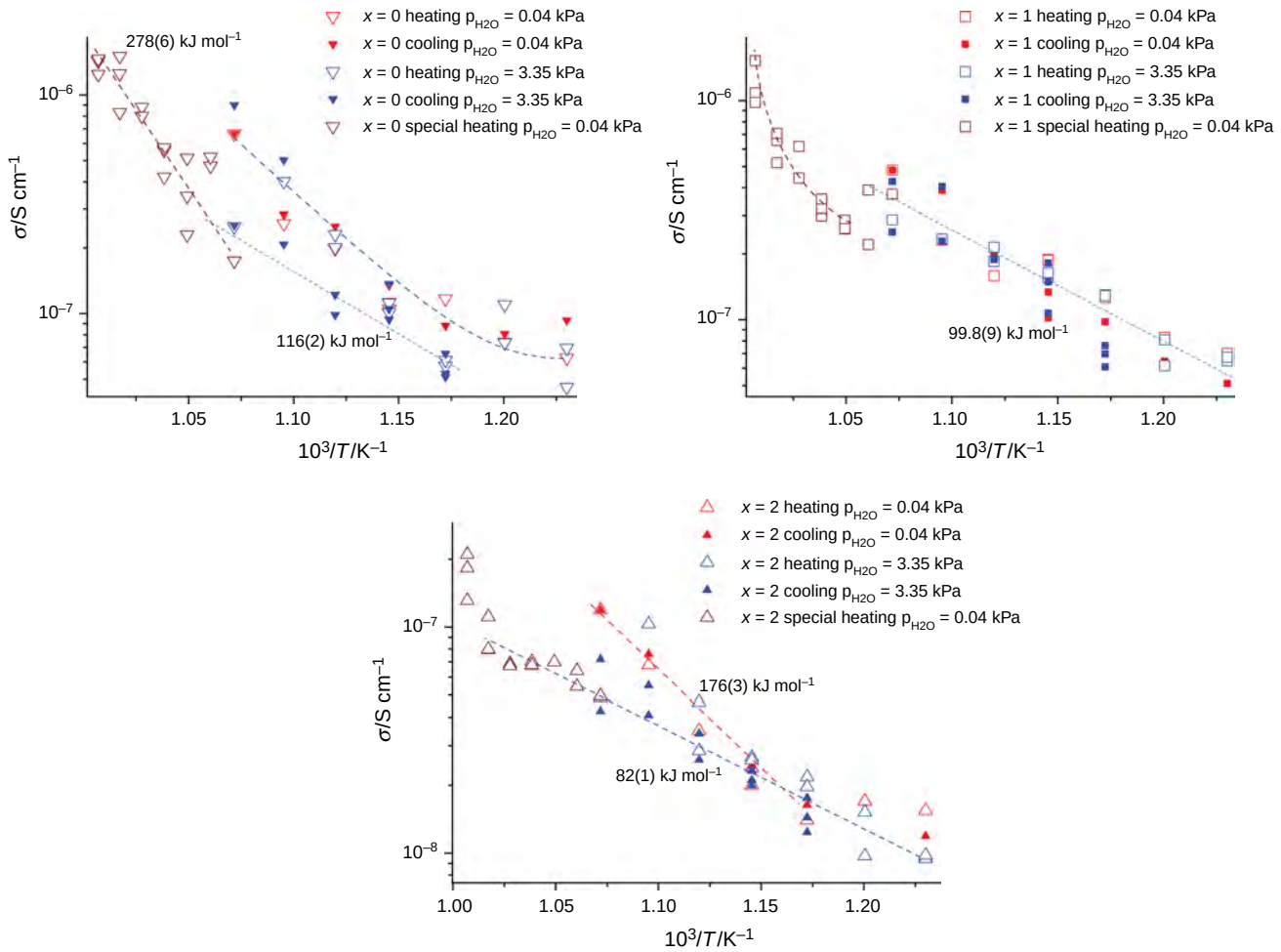

Fig. 7 Electrical conductivity curves of $Ca_5Mg_{4-x}Zn_x(VO_4)_6$ ($0 \le x \le 2$) in the temperature range of 540–660 °C cooling and heating cycles and from 660 to 720 °C special heating

studied low electrical conductivity of such an anti-zeolitic material as mayenite is the interaction of the surface of the material with water vapor from the atmosphere with decay into insulating phases $CaAl_2O_4$ and $Ca_3Al_2O_6$ [13].

Dilatometric curves demonstrate that samples may be easily deformed above 700 °C under static load. Samples are always clamped by the holder in impedance cell during the measurements. Given the above-listed observations, electrical conductivity measurements above 660 °C are arranged by alternative technique to avoid the contribution of inelastic deformation. Obtained results make evident that the resistivity decreases. However, whether the change in the geometry of the samples affected the result or the change in the defect structure remains unclear and requires more detailed revision.

The highest value of electrical conductivity is observed equal 1.5×10^{-6} S/cm at 720 °C for $Ca_5Mg_4(VO_4)_6$. This value is common for dielectric materials and is hence specific for garnet-related crystals. Isomorphous substitution of Mg^{2+} with Zn^{2+} causes the decreasing of electrical conductivity.

Conclusions

Thermal stability and electrical conductivity of $Ca_5Mg_{4-x}Zn_x(VO_4)_6$ ($0 \le x \le 4$) calcium vanadates are studied for the first time using simultaneous thermal analysis, dilatometry and impedance spectroscopy. The data on the thermal behavior, shrinkage processes and the coefficients of thermal expansion values were obtained. The onset of melting process of $Ca_5Mg_{4-x}Zn_x(VO_4)_6$ ($0 \le x \le 4$) decreases with increasing content of Zn^{2+}, whereas the coefficient of thermal expansion increases. CTE hysteresis is demonstrated in its thermal dependence. The solid solution demonstrates low electrical conductivity of about 10^{-6} S/cm which is specific for garnet-related crystals. The value of electrical conductivity does not depend on air

humidity; it decreases in $Ca_5Mg_{4-x}Zn_x(VO_4)_6$ ($1 \leq x \leq 4$) with x increasing.

Acknowledgements The reported study was funded by the RFBR according to the research Project No. 17–03–01280. Powder diffraction experiments were carried out in the Shared Access Centre at the IHTE UB RAS.

References

1. Huang Y, Yu YM, Tsuboi T, Seo HJ. Novel yellow-emitting phosphors of $Ca_5M_4(VO_4)_6$ (M = Mg, Zn) with isolated VO_4 tetrahedra. Opt Express. 2012;20(4):4360–8.
2. Pavitra E, Raju GSR, Park JY, Wang L, Moon BK, Yu JS. Novel rare-earth-free yellow $Ca_5Zn_{3.92}In_{0.08}(V_{0.99}Ta_{0.01}O_4)_6$ phosphors for dazzling white light-emitting diodes. Sci Rep. 2015. https://doi.org/10.1038/srep10296.
3. Yao G, Liu P, Zhang H. Novel series of low-firing microwave dielectric ceramics: $Ca_5A_4(VO_4)_6$ (A^{2+} = Mg, Zn). J Am Ceram Soc. 2013;96(6):1691–3.
4. Wang D, Xiang H, Tang Y, et al. A low-firing Ca5Ni4(VO4)6 ceramic with tunable microwave dielectric properties and chemical compatibility with Ag. Ceram Int. 2016;42:15094–5.
5. Xiang H, Fang L, Jiang X, Li C. Low-firing and microwave dielectric properties of $Na_2YMg_2V_3O_{12}$ ceramic. Ceram Int. 2016;42:3701–5.
6. Xiang H, Tang Y, Fang L, Porwal H, Li C. A novel ultra-low temperature cofired $Na_2BiZn_2V_3O_{12}$ ceramic and its chemical compatibility with metal electrodes. J Mater Sci Mater Electron. 2016. https://doi.org/10.1007/s10854-016-5689-5.
7. Müller-Buschbaum HK, Postel M. Eine weitere oxovanadatphase mit Granatstruktur: $Ca_5Mg_3ZnV_6O_{24}$. Z Anorg Allg Chem. 1992;615:101–3.
8. Gfeller F. Mayenite $Ca_{12}Al_{14}O_{32}[X^{2-}]$: from minerals to the first stable electride crystals: highlights in mineralogical crystallography/Thomas Armbruster; Rosa Micaela Danisi. Berlin: de Gruyter; 2016.
9. Galuskin E, Gfeller F, Galushkina IO, Armbruster T, Bailau R, Sharygin VV. Mayenite supergroup, part I: recommended nomenclature. Eur J Mineral. 2015;27:99–111.
10. Hosono H, Hayashi K, Kajihara K, Sushko P, Shluger A. Oxygen ion conduction in $12CaO{\cdot}7Al_2O_3$: O^{2-} conduction mechanism and possibility of O^- fast conduction. Solid State Ion. 2009;180:550–6.
11. Lide DR, editor. CRC handbook of chemistry and physics. 84th ed. Boca Raton: CRC Press; 2003. p. 4–93.
12. Dhar R, Pandey RS, Srivastava SL. Applicability of Van't Hoff equation in calculation of impurities in liquid crystalline materials. Indian J Pure Appl Phys. 2002;40:42–4.
13. Eufinger JP, Schmidt A, Lerch M, Janek J. Novel anion conductors—conductivity, thermodynamic stability and hydration of anion substituted mayenite-type cage compounds C12A7: X (X = O, OH, Cl, F, CN, S, N). Phys Chem Chem Phys. 2015;17:6844–57.